



ISTITUTO NAZIONALE DI RICERCA METROLOGICA Repository Istituzionale

Specific risks of false decisions in conformity assessment of a substance or material with a mass balance constraint – A case study of potassium iodate

This is the author's submitted version of the contribution published as:

Original

Specific risks of false decisions in conformity assessment of a substance or material with a mass balance constraint – A case study of potassium iodate / Pennechi, Francesca R.; Kuselman, Ilya; Di Rocco, Aglaia; Brynn Hibbert, D.; Sobina, Alena; Sobina, Egor. - In: MEASUREMENT. - ISSN 0263-2241. - 173:(2021), p. 108662. [10.1016/j.measurement.2020.108662]

Availability:

This version is available at: 11696/73030 since: 2022-02-16T18:02:14Z

Publisher:

ELSEVIER SCI LTD

Published

DOI:10.1016/j.measurement.2020.108662

Terms of use:

This article is made available under terms and conditions as specified in the corresponding bibliographic description in the repository

Publisher copyright

(Article begins on next page)

Measurement

Specific risks of false decisions in conformity assessment of a substance or material with a mass balance constraint – A case study of potassium iodate --Manuscript Draft--

Manuscript Number:	
Article Type:	Research Paper
Keywords:	Conformity assessment; Mass balance constraint; Bayesian multivariate modelling; Monte Carlo method; Specific risks; Potassium iodate
Corresponding Author:	Ilya Kuselman, D.Sc. Independent Consultant on Metrology Modiin, ISRAEL
First Author:	Francesca R. Pennechi
Order of Authors:	Francesca R. Pennechi Ilya Kuselman Aglaia Di Rocco D. Brynn Hibbert Alena Sobina Egor Sobina
Abstract:	<p>A methodology for the Bayesian evaluation of total specific risks of false decisions on conformity of a substance or material due to measurement uncertainty was developed using Monte Carlo simulations, taking into account the mass balance constraint of the data. As a case study, the results of testing a potassium iodate batch, considered as a candidate reference material of potassium iodate purity, were analyzed and discussed for different models of the prior probability density function and the likelihood function. Different scenarios of the risks related to determination of potassium iodate purity were studied, when the direct or indirect test method is applied, as well as when both are used simultaneously. The scenario without the closure operation for the measured values (but with the mass balance constraint for the corresponding actual/"true" values) was the most informative concerning the influence of the measured values and associated measurement uncertainties on the risks.</p>

Cover letter

Professor Paolo Carbone,
Editor-in Chief, Measurement

23 July, 2020

Dear Prof. Carbone,

Please find attached the manuscript by Francesca R. Pennechi, Ilya Kuselman, Aglaia Di Rocco, D. Brynn Hibbert, Alena Sobina and Egor Sobina, titled "Specific risks of false decisions in conformity assessment of a substance or material with a mass balance constraint – A case study of potassium iodate", which we would like to publish in Measurement.

Novelty Statement: A methodology for the Bayesian evaluation of total specific risks of false decisions on conformity of a substance or material due to measurement uncertainty is developed using Monte Carlo simulations, taking into account the mass balance constraint of the data. As a case study, the results of testing a potassium iodate batch, considered as a candidate reference material of potassium iodate purity, are analyzed and discussed for different models of the prior probability density function and likelihood function.

Declaration of interest: There is no any actual or potential conflict of interest of any author.

Submission declaration and verification: The work described has not been published previously, it is not also under consideration for publication elsewhere. The publication in Measurement is approved by all the authors.

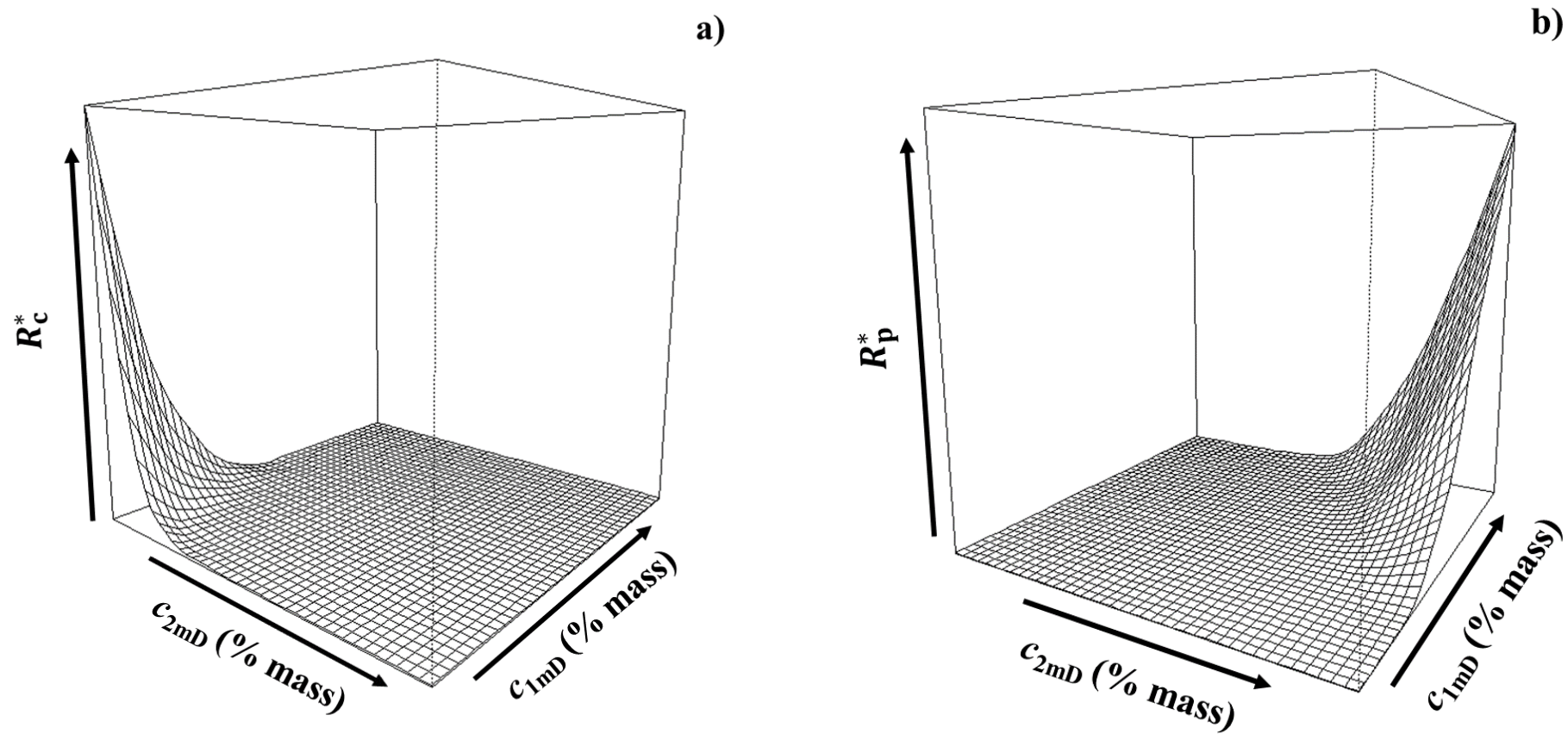
Best regards,



Dr. Ilya Kuselman,
the manuscript corresponding author,
ilya.kuselman@gmail.com
ilya.kuselman@bezeqint.net

HIGHLIGHTS

- Specific risks in a material conformity assessment are studied at a mass balance constraint
- A Bayesian evaluation of total specific risks due to measurement uncertainty is developed
- A Monte Carlo method taking into account the mass balance constraint is applied
- Specific risks in the assessment of a potassium iodate purity are evaluated as a case study



Total specific consumer's risk R_c^* (a) and producer's risk R_p^* (b) in dependence on measured directly purity c_{1mD} and impurities content c_{2mD} .

Specific risks of false decisions in conformity assessment of a substance or material with a mass balance constraint – A case study of potassium iodate

Francesca R. Pennechi^a, Ilya Kuselman^{b,*}, Aglaia Di Rocco^c, D. Brynn Hibbert^d,
Alena Sobina^e and Egor Sobina^e

^a Istituto Nazionale di Ricerca Metrologica (INRIM), Strada delle Cacce 91, 10135 Turin, Italy

^b Independent Consultant on Metrology, 4/6 Yarehim St., 7176419 Modiin, Israel

^c University of Turin, Via Verdi 8, 10124, Turin, Italy

^d School of Chemistry, UNSW Sydney, Sydney NSW 2052, Australia

^e Ural Research Institute for Metrology - Affiliated Branch of D.I. Mendeleev Institute for Metrology (VNIIM-UNIIM), Krasnoarmeyskaya 4, 620000 Ekaterinburg, Russia

* Corresponding author. Tel.: +972-50-6240466

E-mail address: ilya.kuselman@bezeqint.net (I. Kuselman).

4/6 Yarehim St., Modiin, 7176419 Israel

ABSTRACT

A methodology for the Bayesian evaluation of total specific risks of false decisions on conformity of a substance or material due to measurement uncertainty was developed using Monte Carlo simulations, taking into account the mass balance constraint of the data. As a case study, the results of testing a potassium iodate batch, considered as a candidate reference material of potassium iodate purity, were analyzed and discussed for different models of the prior probability density function and the likelihood function. Different scenarios of the risks related to determination of potassium iodate purity were studied, when the direct or indirect test method is applied, as well as when both are used simultaneously. The scenario without the closure operation for the measured values (but with the mass balance constraint for the corresponding actual/“true” values) was the most informative concerning the influence of the measured values and associated measurement uncertainties on the risks.

Keywords:

Conformity assessment; Mass balance constraint; Bayesian multivariate modelling; Monte Carlo method; Specific risks; Potassium iodate

1. Introduction

Three models of prior probability density function (pdf) and likelihood function (likelihood), describing a chemical composition of a multicomponent substance or material which is subject to a mass balance constraint, were applied in the framework of a Bayesian multivariate approach to conformity assessment in ref. [1]. The prior pdf (prior) expresses information about the substance or material that is accumulated before testing of its current item - batch, lot or environmental compartment, while likelihood characterizes the new information obtained from the item test/measurement. Modeling these functions by means of truncated normal distributions of the components' contents and a closure operation (normalizing the contents sum according to the mass balance constraint) allows evaluating risks of false decisions in conformity assessment. Model 1 is suitable for materials whose composition is measured completely, i.e. contents of all the components under test are measured using the appropriate physicochemical methods. Model 2 can be applied for testing substances or materials in which the main component content is not measured using physicochemical methods, but is calculated based on a mass balance constraint. Model 3 is a helpful tool for understanding sources of experimental correlation between the measured components' contents, disentangling the so-called spurious part, caused by the mass balance constraint, from natural and/or technological correlations. A Monte Carlo method, coded in the R programming environment, was developed for calculations of the coverage probability of the multivariate prior and the *total global* risks (consumer's and producer's [2]) of false decisions on conformity of a substance or material due to measurement uncertainty, taking into account the mass balance constraint of the data [1]. These risks are the probabilities of incorrect conformity assessment of an item randomly drawn from a statistical population of such items, when two or more component contents are under test. A total global risk characterizes the conformity assessment of a substance or material globally. It can also be interpreted as the probability of a false decision on conformity of two or more tested components' contents in a future item, assuming that conditions of the substance or material production and testing will not change [3]. For a specific item under test, the total risks are referred to as the *total specific* consumer's risk (probability that a specific accepted item does not conform) and the *total specific* producer's risk (probability that a specific rejected item actually conforms) [4].

The aim of the present paper is the evaluation of total specific risks of false decisions on conformity of a substance or material due to measurement uncertainty, taking into account the mass balance constraint of the data. As a case study, results from the Ural Research Institute for Metrology (UNIIM) [5] of testing a specific potassium iodate batch, being considered as a candidate reference material [6] of potassium iodate purity, are analyzed and discussed using the models of the prior and likelihood developed in [1].

2. Evaluation of specific risks for multicomponent material or object

Bayes' theorem for the multivariate pdf of components' contents of a multicomponent material or object is expressed by the following equation:

$$g(\mathbf{c} | \mathbf{c}_m) = C g_0(\mathbf{c}) h(\mathbf{c}_m | \mathbf{c}), \quad (1)$$

where $\mathbf{c} = [c_1, c_2, \dots, c_n]$ and $\mathbf{c}_m = [c_{1m}, c_{2m}, \dots, c_{nm}]$ are vectors of the actual ("true") values c_i and measured values c_{im} , respectively, $i = 1, 2, \dots, n$; $g(\mathbf{c} | \mathbf{c}_m)$ is the multivariate posterior pdf; C is a normalizing constant; $g_0(\mathbf{c})$ is the multivariate prior pdf; and $h(\mathbf{c}_m | \mathbf{c})$ is the multivariate likelihood function taking into account the measurement uncertainties and possible covariances between c_{im} . The product $g_0(\mathbf{c}) h(\mathbf{c}_m | \mathbf{c})$ is the multivariate joint pdf of actual values \mathbf{c} and the measured values \mathbf{c}_m . Eq. (1) takes into account possible correlations between actual values of the contents of the components and/or between their measured values [1, 3].

The total specific consumer's risk, when all measured values c_{im} are within their acceptance intervals A_i , is

$$R_c^* = 1 - \int_{T_1} \dots \int_{T_n} g(\mathbf{c} | \mathbf{c}_m) d\mathbf{c}, \quad (2)$$

where T_i is the tolerance (specification) interval of c_i , and $T = T_1 \times T_2 \times \dots \times T_n$ is the tolerance domain for vector \mathbf{c} .

The total specific producer's risk, when ν of n contents measured values c_{im} , with $1 \leq \nu \leq n$, are outside their acceptance intervals A_i (i.e. out of the acceptance domain $A = A_1 \times A_2 \times \dots \times A_n$ for vector \mathbf{c}_m), is

$$R_p^* = \int_{T_1} \dots \int_{T_\nu} \int_0^\infty \dots \int_0^\infty g(\mathbf{c} | \mathbf{c}_m) d\mathbf{c}, \quad (3)$$

where, without losing generality, the measured values which are outside their acceptance intervals are the first ν .

In the univariate case, when only a particular component content is considering for conformity assessment, for example the main component content c_1 , the particular specific consumer's risk $R_{c_1}^*$ and the particular specific producer's risk $R_{p_1}^*$ are the following, according to JCGM 106 [2]:

$$R_{c_1}^* = \int_0^{T_{L1}} g(c_1 | c_{1m}) dc_1 = \frac{\int_0^{T_{L1}} g_0(c_1) h(c_{1m} | c_1) dc_1}{\int_0^{100} g_0(c_1) h(c_{1m} | c_1) dc_1} \quad (4)$$

for $c_{1m} > T_{L1}$, where T_{L1} is the lower tolerance limit of the component content, and

$$R_{p_1}^* = \int_{T_{L1}}^{100} g(c_1 | c_{1m}) dc_1 = \frac{\int_{T_{L1}}^{100} g_0(c_1) h(c_{1m} | c_1) dc_1}{\int_0^{100} g_0(c_1) h(c_{1m} | c_1) dc_1} \quad (5)$$

for $c_{1m} < T_{L1}$, when the lower tolerance and acceptance limits coincide.

3. Material and test methods

A purchased batch of synthesized potassium iodate (KIO_3), produced by Acros Organics [7], and weighed 1.5 kg, was divided at UNIIM in 145 vials, about 10 g in each vial. Twelve vials from 145 were used for the batch homogeneity study with the purity direct measurement method (Sec. 3.2.1) according to ISO Guide 35 [6]. The standard deviation of the potassium iodate purity caused by the batch inhomogeneity was 0.003 %. The same standard deviation of 0.003 % was also

obtained in a year-long stability study. These standard deviations are statistically negligible in comparison with the standard measurement uncertainty of the applied direct method, equal to 0.007 %.

3.1. Specification and acceptance limits

The KIO_3 content/purity c_1 in the batch, expressed as mass fraction of KIO_3 , should not be less than $T_{L1} = 99.9\%$ which is the lower tolerance/specification limit required for a candidate reference material of this type for verification of measuring instruments [8]. The upper tolerance limit (not greater than) of the content c_2 of impurities (the sum of their mass fractions) is, accordingly, $T_{U2} = (100 - 99.9)\% = 0.1\%$. The reference material is planned also for use in quality control of potassium iodate according to the standard [9], which sets the lower specification limit of purity at 99.8 % for “Chemically pure” and “Pure for chemical analysis” grades of the salt. The impurities which should be under control by this standard are substances insoluble in water; nitrogen-containing compounds; iodide and free iodine; sulfates; chlorides, bromides and chlorates; iron; heavy metals; and sodium.

The acceptance limits for test results of a candidate reference material of potassium iodate are not set in the regulation [8], and in practice the tolerance/specification limits are used instead. In other words, acceptance limits are coincidental here with tolerance limits, i.e. $A = T$.

3.2. Methods for testing a candidate reference material

Two test methods, direct and indirect [6], were used for the determination of purity, i.e. for measuring the actual (“true”) potassium iodate content c_1 .

3.2.1. Direct method

The direct method is based on the SI-traceable, primary coulometric titration of oxidants, expressed as mass of potassium iodate, using a vertical coulometric cell and amperometric end-point detection with two polarized electrodes. The measurement procedure consists of the following steps: 1) coulometric standardization of sodium thiosulfate by electrogenerated iodine,

2) reaction of an excess of standardized sodium thiosulfate with iodine released by a potassium iodate test portion of 0.15 g from acidified potassium iodide solution, 3) coulometric titration of the sodium thiosulfate excess by electrogenerated iodine, and 4) calculation of c_{1mD} (subscript 'm' means measured value, and 'D' – direct method), as well as evaluation of the associated measurement uncertainty. More about the method and measurement uncertainty components is available in the publications [10, 11].

The mean measured value was $c_{1mD} = 99.966\%$ with associated combined standard measurement uncertainty $u_{1D} = 0.007\%$.

3.2.2. Indirect method

The indirect method is based on the mass balance approach and measurement of the content of the impurities, as described in ISO Guide 35 [6] and in a number of publications on applications of this approach, in particular for inorganic substances or materials [12-15]:

$$c_{1mI} = 100 - c_{2mD}, \quad (6)$$

where subscript 'I' means indirect method, and c_{2mD} is the measured content value of the impurities as sum of mass fractions of the elements in their assumed chemical (ionic) form, including mass fraction of the potassium ion excess due to non-stoichiometry.

A test portion of 0.5 g was used for measurement of elemental mass fractions of impurities by standard mode inductively coupled plasma mass spectrometry (ICP-MS), and a 1.0 g test portion - for ionic impurities by ion chromatography (IC). Substances insoluble in water were not detected. Iodide ions and free iodine, nitrogen containing nitrite and nitrate ions, as well as chlorates, were not detected also and not taken into further account. Mass fractions of seventy-one impurities were measured. Fourteen of them (mass fractions of Na, Mg, Al, Ca, Ti, Fe, Ni, Cu, Zn, Rb, Sr, Cd, Ba, and Bi) were quantified with ICP-MS. The mass fractions of another fifty-four elements were equal or less than their corresponding ICP-MS limits of detection (LOD). In this case, LOD/2 were taken as the estimates of the mass fractions, according to Guide [14]. Mass fractions of SO_4^{2-} and Cl^- ions were measured by IC. The potassium excess was evaluated using the concept of

electroneutrality of an ion system: the system should maintain equality of positive and negative charges [16-18].

The mean measured content of the impurities was $c_{2mD} = 0.025$ %. The purity calculated by Eq. (6) was $c_{1mI} = 99.975$ %. No correlation was observed between measured values of the impurities' mass fractions. The combined standard measurement uncertainty associated with \mathbf{c}_{2mD} and c_{1mI} , calculated by Guides [6] and [15], was $u_{2D} = 0.005$ %.

4. Modelling and calculation for the mass balance constraint

4.1. Prior pdfs

There are two quantities measured in the batch testing: 1) the potassium iodate content/purity c_1 as mass fraction, %, and 2) the content c_2 of impurities as the sum of their mass fractions, %.

The prior pdf for the purity $g_0(\mathbf{c}_1)$ is approximated by a univariate truncated normal distribution $TN(\mu_1, \sigma_1)$ on the interval [0 %, 100 %]:

$$g_0(c_1) = \frac{\phi\left(\frac{c_1 - \mu_1}{\sigma_1}\right)}{\sigma_1 \left(\Phi\left(\frac{100 - \mu_1}{\sigma_1}\right) - \Phi\left(\frac{-\mu_1}{\sigma_1}\right) \right)}, \quad (7)$$

where location parameter $\mu_1 = 99.95$ % is the mean of the permissible purity interval [99.9 %, 100 %] by regulation [8] and scale parameter $\sigma_1 = 0.015$ % is the standard deviation of a batch purity, assumed equal to the target (standard) measurement uncertainty [8, 19]; $\phi(\cdot)$ is the pdf of the standard normal distribution and $\Phi(\cdot)$ is its cumulative distribution function. Note that in the present study the scale parameter does not characterize variability of conditions of a batch production [3], but reflects the variability of selection of raw material appropriate for development of the reference material.

A histogram (numerical representation) of the prior pdf $g_0(c_1)$ is shown in Fig. 1a; outside the interval [0 %, 100 %], it is equal to zero. Truncation at 100 % slightly influences this pdf because of the small scale value; the distribution is however skewed to the left.

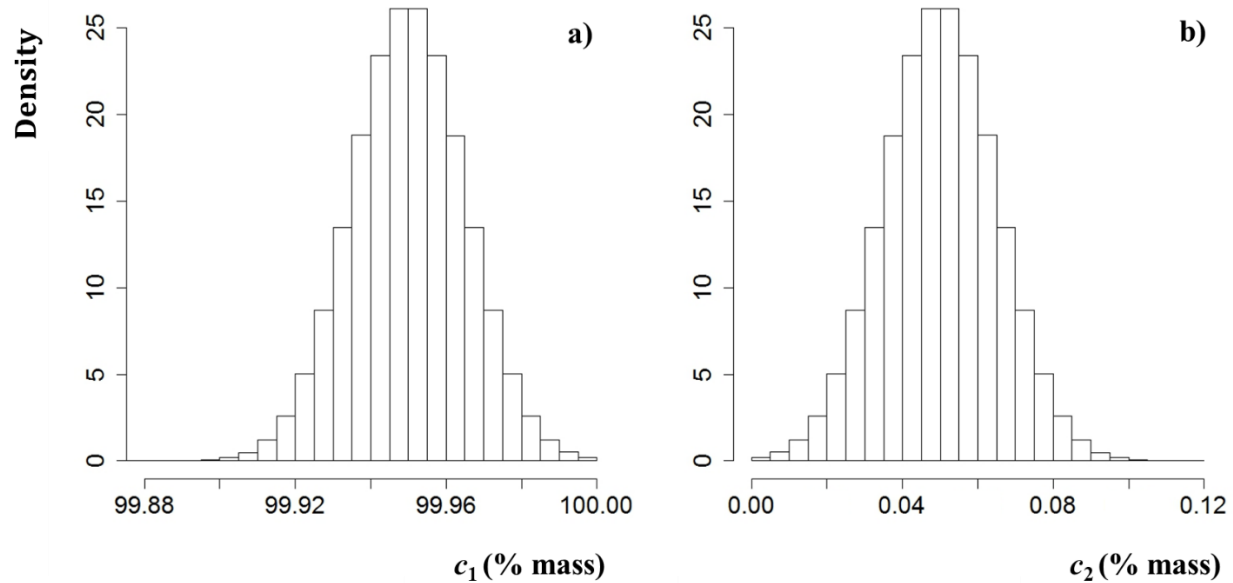


Fig. 1. Histograms of the purity prior pdf (a) and the impurities content prior pdf (b). The ordinates are densities; abscises in (a) and (b) are purity c_1 % mass and impurities content c_2 % mass, respectively. The location and scale parameters of the purity pdf are $\mu_1 = 99.95$ % and $\sigma_1 = 0.015$ %, respectively.

Because of the mass balance constraint, for each value c_1 of the purity, simulated by randomly sampling from $TN(\mu_1, \sigma_1)$, a corresponding content value c_2 of the impurities is deterministically evaluated as $c_2 = 100 - c_1$. This approach follows Model 2 for prior pdfs described in ref. [1, sec. 2.3]. Incidentally, for just two involved variables, this model degenerates into the sequential Model 3. The histogram of the prior pdf for impurities content c_2 is presented in Fig. 1b. This distribution (depicted on the c_2 range [0 %, 0.12 %], complementary to the c_1 range [99.88 %, 100 %]) is the specular reflection of that in Fig. 1a. Hence, the probability for c_2 values to be greater than $T_{U2} = 0.1$ % is the same as that for c_1 values to be smaller than $T_{L1} = 99.9$ %.

4.2. Likelihood

There are two tasks of the evaluation of specific risks and corresponding two scenarios of likelihood modelling:

1) Both contents of purity and impurities are under conformity assessment. One of the two quantities is measured directly, while the other is recovered from the former through the mass balance constraint.

1a) Purity c_{1mD} is measured directly, while content of the impurities is evaluated as $c_{2mI} = 100 - c_{1mD}$. In this scenario, the likelihood for c_{1mD} is modelled by a truncated normal distribution on $[0 \%, 100 \%,]$, with location parameter equal to the actual “true” value c_1 and scale parameter equal to measurement uncertainty u_{1D} . This modelling follows Model 2 for likelihood functions described in ref. [1, sec. 2.4].

1b) Purity c_{1mI} is evaluated indirectly from the measured content c_{2mD} of the impurities, i.e. $c_{1mI} = 100 - c_{2mD}$. The likelihood for c_{2mD} is modelled by a truncated normal distribution on $[0 \%, 100 \%,]$, with location parameter equal to the actual “true” value c_2 and scale parameter equal to measurement uncertainty u_{2D} . This modelling follows also Model 2 as in the scenario 1a) above.

2) Both c_{1mD} and c_{2mD} are measured directly (and independently), and both undergo the conformity assessment. For modelling their likelihood function, the univariate truncated normal distributions $TN(c_1, u_{1D})$ and $TN(c_2, u_{2D})$ on the interval $[0 \%, 100 \%,]$ are considered, respectively, and then the corresponding simulated values $\mathbf{c}_m = [c_{1mD}, c_{2mD}]$ are closed according to the closure operation in order for them to satisfy the mass balance constraint:

$$clo(\mathbf{c}_m) = \left[\frac{100 c_{1mD}}{c_{1mD} + c_{2mD}}, \frac{100 c_{2mD}}{c_{1mD} + c_{2mD}} \right]. \quad (8)$$

Note, the closure operation leads to a perfect negative correlation between c_{1mD} and c_{2mD} values, with the Pearson correlation coefficient of -1 . In the case where c_{1mD} and c_{2mD} values are not mandatorily satisfying the mass balance constraint, the closure operation (8) can be avoided. Such a situation is possible when the sum of c_{1mD} and c_{2mD} is less than 100 %, because not all the impurities are detected, or greater than 100 % due to measurement uncertainties associated with the measured values.

A scenario when the directly-measured purity c_{1mD} is the only quantity under conformity assessment (a univariate task), is also discussed for further comparison.

4.3. Posterior pdf

The posterior distribution describing post-measurement knowledge about property values of a component is expressed in Eq. (1) as $g(\mathbf{c} | \mathbf{c}_m)$. In the current study, it is the pdf of actual content values of the potassium iodate and impurities given their corresponding measured values in the batch. This pdf is the normalized product of the prior and the likelihood. It allows to calculate the total specific consumer's risks by Eq. (2) and the total specific producer's risks by Eq. (3). In the univariate case, the particular specific consumer's risks were calculated by Eq. (4) and the particular specific producer's risk - by Eq. (5). The integrals in these equations were evaluated using numerical methods.

4.4. Computational details

4.4.1. Univariate scenario

Modeling of prior $g_0(c_1)$ and likelihood $h(c_{1mD} | c_1)$, based on truncated normal distributions, followed that described for c_1 in Sec. 4.1 and for c_{1mD} in Sec. 4.2, scenario 1a, respectively. Integrals in Eqs. (4) and (5) were evaluated by means of the R "integrate" function for adaptive quadrature of one-dimensional functions [20].

4.4.2. Bivariate scenarios

For scenario 1a in Sec. 4.2, it is worth noting that the total consumer's risk coincides with the particular consumer's risk relevant to the measured directly purity c_{1mD} . When $c_{1mD} > T_{L1}$, corresponding content of impurities calculated as $c_{2mI} = 100 - c_{1mD}$ is smaller than T_{U2} , and the candidate reference material is conforming regulations [8]. The total risk that this material is actually not conforming is equal to one minus the probability that both the actual (posterior) values $c_1 | c_{1mD}$ and $c_2 | c_{2mI}$ are within their corresponding tolerance limits as shown, in Eq. (2). However, $c_1 | c_{1mD} > T_{L1}$ when and only when $c_2 | c_{2mI} < T_{U2}$, by definition of the prior pdf and the likelihood function for the impurities content as 100 % minus the corresponding value of the purity. Therefore, the total specific consumer's risk R_c^* coincides with the particular consumer's risks R_{c1}^* derived in Sec. 4.4.1.

The described reasoning holds as well for the total specific producer's risk R_p^* , hence being equal to R_{p1}^* . The same kind of considerations applies also to scenario 1b. The difference between the risk values in scenarios 1a and 1b is caused just by the difference in uncertainties u_{1D} and u_{2D} associated with the directly measured values of the components' contents.

For scenario 2, where both c_{1mD} and c_{2mD} are measured directly, the total specific risks are calculated according to Eqs. (2) and (3) by means of Monte Carlo (MC) simulation performed in R programming environment. For each specified couple of measured values (c_{1mD} , c_{2mD}), for which the total risk has to be evaluated, integrals of the posterior pdf in Eqs. (2) and (3) involve the ratio of multiple integrals of the joint pdf of vector $[c_1, c_2, c_{1mD}, c_{2mD}]$ with respect to variables c_1 and c_2 over appropriate domains. $M = 10^7$ random vectors $[c_1, c_2, c_{1mD}, c_{2mD}]$ were generated according to the prior modelling for c_1 and c_2 in Sec. 4.1 and the likelihood modelling for c_{1mD} and c_{2mD} in Sec. 4.2, Model 2. A correlation between c_{1mD} and c_{2mD} values is induced by the correlation between actual/"true" values c_1 and c_2 . The induced correlation coefficient is -0.86 : it is weaker than that between c_1 and c_2 (-1), because of the random factors contributing to the measurement uncertainty, which adds noise to the actual values [21].

The above-mentioned integrals are approximated by the number of vectors in which c_1 and c_2 values are in the relevant integration domain and, at the same time, the generated measured values are equal to the specific c_{1mD} and c_{2mD} values, divided by the total number ($M = 10^7$) of generated vectors. Since both integrals in the numerator and denominator of the risk, such as those in Eqs. (4) and (5) for the univariate case, are approximated by a ratio whose denominator is always the same value (i.e., $M = 10^7$), this division is not actually implemented in the code.

Ideally, one should search for those vectors $[c_1, c_2, c_{1mD}, c_{2mD}]$ in which the generated measured values are equal to the specific c_{1mD} and c_{2mD} of interest. However, since the simulation can generate just a finite amount of discrete values, which have a finite numerical representation, the probability to find such vectors is zero, in practice. Therefore, the number of vectors $[c_1, c_2, c_{1mD}, c_{2mD}]$ is counted in which the measured values are encompassed within the range $c_{imD} \pm \varepsilon$, where $\varepsilon = 0.001$ was empirically found to be a sensible tradeoff. This ε value is sufficiently small to be considered as a negligible perturbation with respect to the uncertainties in play, but sufficiently large to allow collecting a good number of vectors both at the numerator and the denominator of the ratios which approximate the risk values.

For a better rendering, risks values in figures related to scenario 2 were smoothed by means of the R “loess” [22] and “loess.surf functions” [23].

The relevant R codes can be sent upon request to the corresponding author.

5. Results and discussion

5.1. Univariate scenario

The particular specific consumer’s risk and producer’s risk, calculated as explained in Sec. 4.4.1, are plotted in Fig. 2a and Fig. 2b, respectively.

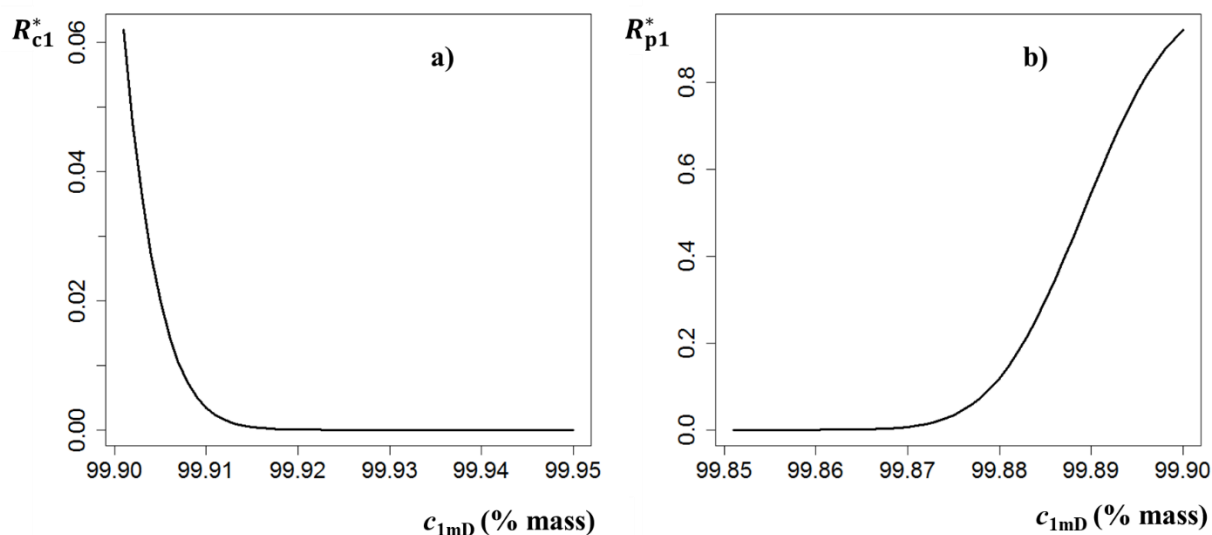


Fig. 2. Dependences of the particular specific consumer’s risk R_{c1}^* (a) and producer’s risk R_{p1}^* (b) on the measured directly purity value c_{1mD} in the univariate scenario. The ordinates are the risks expressed as probabilities in fractions of one, and the abscissae are measured values, % mass.

In the present study, “consumer” is the Regulator (Russian Federation Agency for Technical Regulation and Metrology) defending interests of laboratories which will purchase the reference material, applying the regulation [8]. The consumer’s risk is the probability of the event when the

measured (and certified later) purity value is $c_{1mD} \geq 99.90\%$, while the actual (“true”) value is $c_1 < 99.90\%$. Such actual purity value is not recommended for verification of measuring instruments by the regulation [8] and may cause further problems in a laboratory activity. However, this consumer’s risk shown in Fig. 2a is practically zero, when $c_{1mD} > 99.92\%$.

The risk of “producer” of the reference material (UNIIM) is the probability that the measured purity value is $c_{1mD} < 99.90\%$, when the actual value is $c_1 \geq 99.90\%$. In such case, a false decision of the producer on quality of the raw material and/or its testing is possible, leading to rejection of the material and vain loss of money and time. The producer’s risk illustrated in Fig. 2b decreases to very small values when $c_{1mD} < 99.87\%$: the chance that actual purity value is not less than 99.90% is already negligible.

Replacement of the standard measurement uncertainty $u_{1D} = 0.007\%$ by the standard uncertainty 0.008% of the certified value, combining u_{1D} with the standards deviations of the material inhomogeneity (0.003%) and instability (0.003% also), does not influence the risks values rounded up to hundredth.

By definition, the dependences of the risks on the impurities content are symmetric to the dependences on purity, in this scenario.

5.2. Bivariate scenarios

Scenario 1a is represented in Fig. 3a as the three dimensional dependence of the total specific consumer’s risk R_c^* on c_{1mD} and c_{2mI} . The risk values are shown by vertical navy-blue lines of corresponding length, forming together the risk “wave”. This wave smoothing curve is identical to the curve in Fig. 2a for the univariate scenario in the same intervals of the measured directly purity and the impurities content, measured indirectly. The sky-blue floor of the plot corresponds to zero risk.

The dependence of total specific producer’s risk R_p^* on c_{1mD} and c_{2mI} is presented in Fig. 3b, where the vertical lines showing the R_p^* values form also the risk “wave”, as in Fig. 3a, with the smoothing curve identical to the curve of the univariate scenario in Fig. 2b.

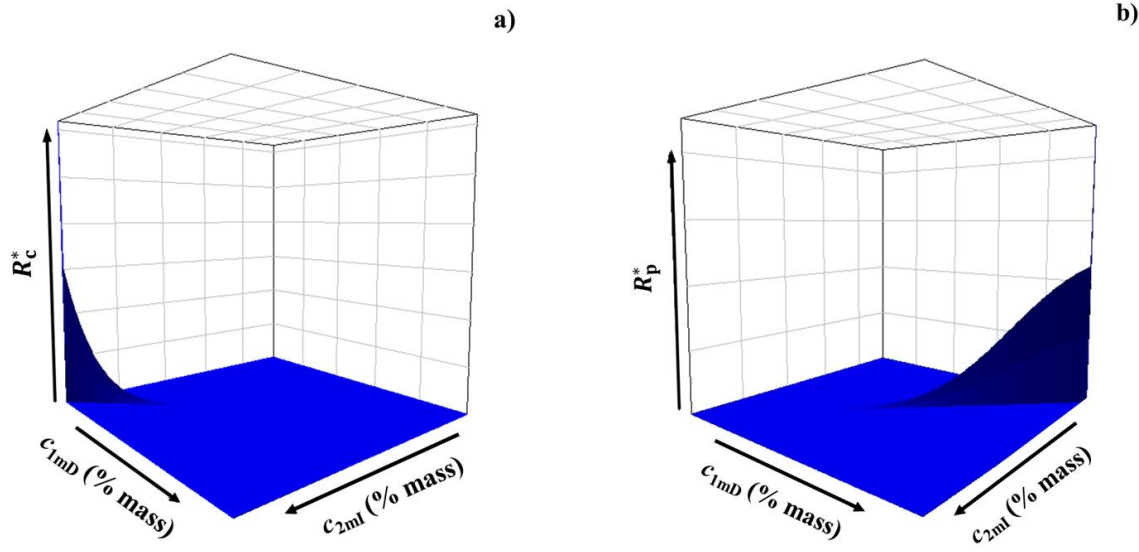


Fig. 3. Total specific consumer's risk R_c^* (a) and producer's risk R_p^* (b) in dependence on measured directly purity c_{1mD} and impurities content c_{2mI} , measured indirectly. Interval of the R_c^* values in plot (a) is $[0, 0.06]$, when $c_{1mD} = [99.90 \%, 99.95 \%]$ and $c_{2mI} = [0.05 \%, 0.10 \%]$. Interval of the R_p^* values in plot (b) is $[0, 0.92]$, when $c_{1mD} = [99.85 \%, 99.90 \%]$ and $c_{2mI} = [0.10 \%, 0.15 \%]$.

The “collapse” of the total risk for two components to the particular risk of one of them is not surprising in the case of compositional data in which one of the two variables (component contents) is modelled exactly as the complement to 100 % of the other: this complementary variable does not convey any further information to the risk evaluation from a probabilistic point of view.

Uncertainty of measured directly purity $u_{1D} = 0.007 \%$ by scenario 1a does not differ significantly from uncertainty of measured indirectly purity by scenario 1b, equal to uncertainty of measured directly impurities content $u_{2D} = 0.005 \%$. Therefore, dependences of the risks on the measured indirectly purity by scenario 1b, are very similar to those shown in Fig. 3. Nevertheless, the risks values may be distinguished: the maximum consumer's risk R_c^* values on the interval of purity $[99.90 \%, 99.95 \%]$, measured directly by scenario 1a and indirectly by scenario 1b, are 0.06 vs. 0.10, respectively. The maximum producer's risk R_p^* values on the interval of purity

[99.85 %, 99.90 %], measured directly by scenario 1a and indirectly by scenario 1b, are 0.92 vs. 0.80, respectively.

Note, although the measurement uncertainty u_{2D} is smaller than u_{1D} , the consumer's risk in scenario 1b is greater than in scenario 1a, whereas the producer's risk is lesser. The reason is that the posterior pdf depends on both the likelihood function (in which the measurement uncertainty is involved as the scale parameter) and the prior pdf. The posterior pdf is characterized by an expectation value lying in between the prior mean and the measured value. At the same measured purity value, e.g. at $c_{1mD} = c_{1mI} = 99.901$ % where the consumer's risk values are the greatest, the (univariate) posterior pdf of c_1 obtained for scenario 1b with $u_{2D} = 0.005$ % is narrower than that for scenario 1a with $u_{1D} = 0.007$ %, as shown in Fig. 4. However, the posterior pdf of scenario 1b is more shifted toward measured value 99.901 %, has a larger tail of the distribution to the left of $T_{L1} = 99.90$ %, and therefore, the consumer's risk is greater here than in scenario 1a.

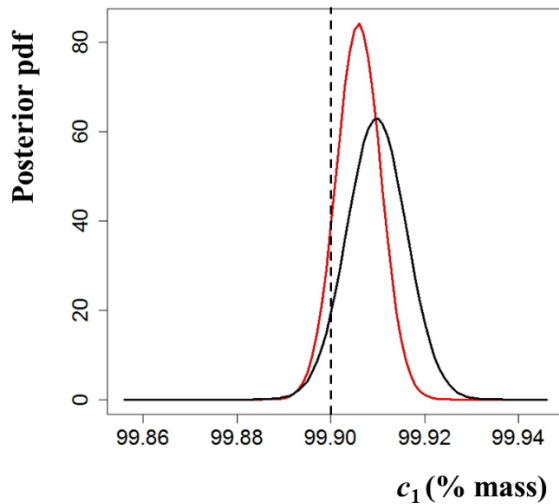


Fig. 4. Posterior pdf of actual purity values c_1 . Black line is the posterior pdf for scenario 1a, red line – for scenario 1b; dotted line is the lower tolerance purity limit T_{L1} .

The total consumer's and producer's specific risks by scenario 2 with the closure operation are demonstrated in Fig. 5, plots a) and b), respectively. The closure operation leads here again to the risk surface collapse into the "waves" as in Fig. 3. These waves in Fig. 5, with maximum values of 0.10 and 0.81 of the consumer's risk and the producer's risk, respectively, are closer to those

obtained in scenario 1b than in scenario 1a. Apparently, the measurement uncertainty u_{2D} , being smaller than u_{1D} , influences the risk values more.

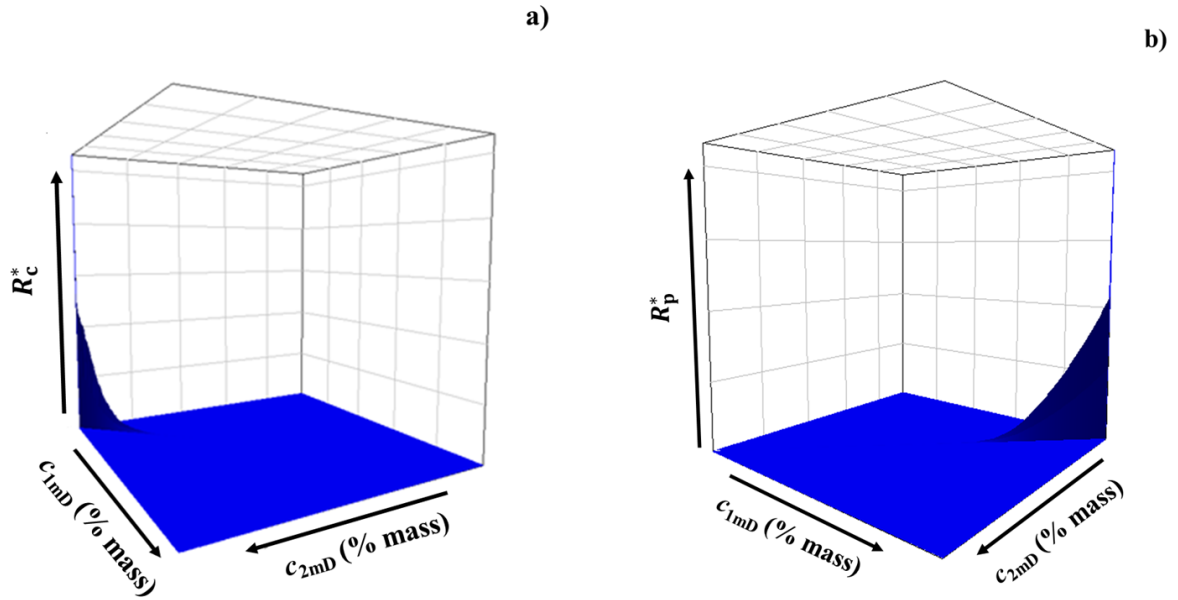


Fig. 5. Total specific consumer's risk R_c^* (a) and producer's risk R_p^* (b) in dependence on measured directly purity c_{1mD} and impurities content c_{2mD} , treated with the closure operation. Interval of the R_c^* values in plot (a) is $[0, 0.10]$, while the interval of the R_p^* values in plot (b) is $[0, 0.81]$. The measured purity and impurities content intervals are as in Fig. 3.

Fig. 6 shows a proper (not degenerate) surface of the consumer's risk (a) and producer's risk (b) when the closure operation is not applied to the measured values. In this case the outcomes of the measurement process, i.e. couples (c_{1mD}, c_{2mD}) in which $c_{1mD} \neq 100 - c_{2mD}$ (whereas $c_1 = 100 - c_2$), are feasible also. The maximum value of the consumer's risk is 0.11, while for the producer's risk it is 0.76.

Note, the maximum risks in Fig. 6, as well as in Fig. 3 and Fig. 5, are related to the shown intervals of the variables, i.e. measured purity and impurities content values. Out of these intervals the risks behavior and their maximum values may change. In particular, the total specific producer's risk in Fig. 6b is zero when $c_{1mD} > 99.90\%$ and $c_{2mD} < 0.10\%$, by definition. However,

this risk may increase when, for example, $c_{1mD} > 99.90\%$ and simultaneously $c_{2mD} > 0.10\%$, or vice versa, when $c_{1mD} < 99.90\%$ and simultaneously $c_{2mD} < 0.10\%$

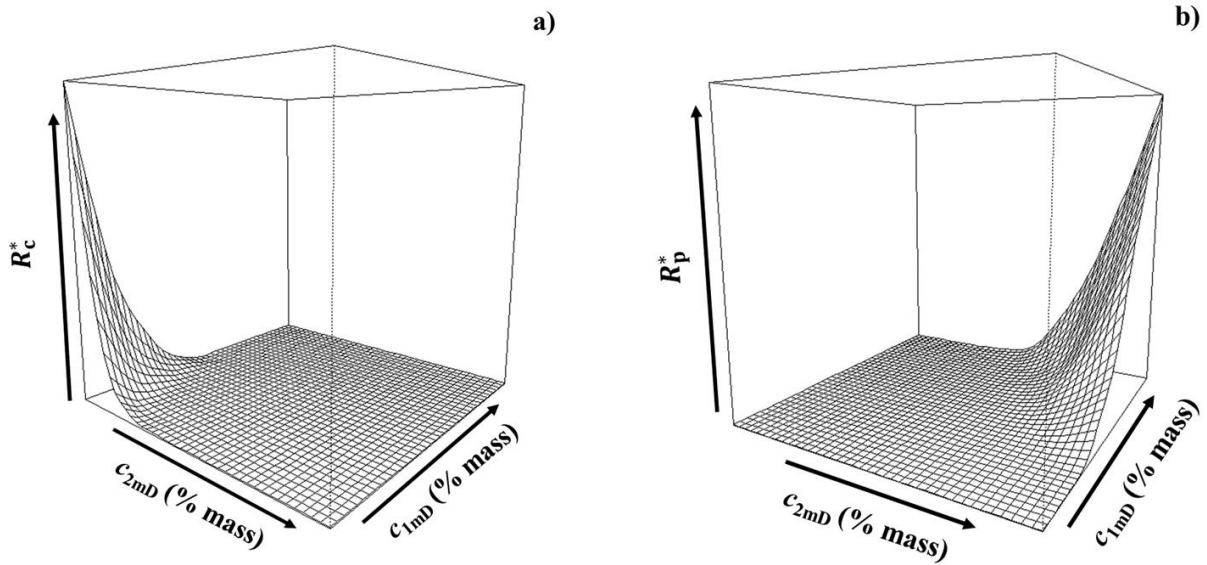


Fig. 6. Total specific consumer's risk R_c^* (a) and producer's risk R_p^* (b) in dependence on measured directly purity c_{1mD} and impurities content c_{2mD} , without closure operation. Interval of the R_c^* values in plot (a) is $[0, 0.11]$, while the interval of the R_p^* values in plot (b) is $[0, 0.76]$. The measured purity and impurities content intervals are as in Fig. 3.

In general, comparing the discussed univariate and bivariate scenarios of the risks related to determination of potassium iodate purity, one can see that practically the same results are obtained in bivariate scenarios, transformed de-facto into univariate cases by the mass balance constraint. This means that there is no significant difference between direct and indirect purity test methods if their measurement uncertainties are approximately equal. Note, the “collapse” of multivariate scenarios into univariate scenarios because of the closure operation, as happens in bivariate scenarios, is impossible for three or more variables.

Bivariate scenario 2 without the closure operation for the measured values (but with the mass balance constraint for actual/“true” values and their prior pdf) does not decrease the risks in comparison to other scenarios. However, this scenario is the most informative concerning the influence of the proper measured values and associated measurement uncertainties on the risks.

By all the scenarios, at the measured values $c_{1mD} = 99.966\%$ and $c_{2mD} = 0.025\%$, reported by UNIIM for the studied batch of potassium iodate as candidate reference material, both the total specific consumer's risk and the total producer's risk are essentially zero.

6. Conclusions

A methodology for the Bayesian evaluation of total specific risks of false decisions on conformity of a substance or material due to measurement uncertainty is developed using Monte Carlo simulations, taking into account the mass balance constraint of the data. As a case study, the results of testing a potassium iodate batch, considered as a candidate reference material of potassium iodate purity, were analyzed and discussed for different models of the prior pdf and likelihood function.

Comparing the studied scenarios of the risks related to determination of purity of a potassium iodate batch, it was shown that practically the same results are obtained, when the direct and indirect purity test methods are used, if their measurement uncertainties are approximately equal. That is caused by the “collapse” of the bivariate scenarios (modelling both the purity and the impurities content) into corresponding univariate cases modelling just the purity. This is an effect of the mass balance constraint applied by means of the closure operation to the measured values of just two quantities.

The bivariate scenario without application of the closure operation to the measured values (but with the mass balance constraint for actual/“true” values) is the most informative concerning the influence of the measured values and associated measurement uncertainties on the risks.

By all the scenarios, however, at the measured values $c_{1mD} = 99.966\%$ and $c_{2mD} = 0.025\%$, reported for the studied batch of potassium iodate as candidate reference material, both the total specific consumer's risk and producer's risk are essentially zero.

CRediT authorship contribution statement

Francesca R. Pennecchi: Methodology, Visualization, Formal analysis, Software, Writing – Reviewing and editing; **Ilya Kuselman:** Conceptualization, Project administration, Writing -

Original draft preparation; **Aglaia Di Rocco**: Software, Data curation; **D. Brynn Hibbert**: Writing – Reviewing and editing; **Alena Sobina**: Resources: Provision of raw data; **Egor Sobina**: Validation.

Declaration of Competing Interest

The authors declare that they have no known competing financial interests or personal relationships that could have appeared to influence the work reported in this paper.

Acknowledgements

This research was supported in part by the International Union of Pure and Applied Chemistry (IUPAC Project 2019-012-1-500).

The authors would like also to thank coworkers of UNIIM, Russia: A.Yu. Shimolin, performed the coulometric titration and ion-chromatographic measurements, and T.N. Tabachnikova, carried out the ICP-MS measurements, mentioned in the present paper.

References

- [1] F.R. Pennechi, A. Di Rocco, I. Kuselman, D.B. Hibbert, M. Segal, Correlation of test results and influence of a mass balance constraint on risks in conformity assessment of a substance or material, *Measurement* 163C (2020) 107947. <http://dx.doi.org/10.1016/j.measurement.2020.107947>.
- [2] JCGM 106, Evaluation of Measurement Data – The Role of Measurement Uncertainty in Conformity Assessment, 2012. <http://www.bipm.org/en/publications/guides/> (accessed 6 May 2020).
- [3] I. Kuselman, F.R. Pennechi, R.J.N.B. da Silva, D.B. Hibbert, IUPAC/CITAC Guide: Evaluation of risks of false decisions in conformity assessment of a multicomponent material or object (IUPAC Technical Report), *Pure Appl Chem* 92 (2020) Accepted 14 June 2020. <http://dx.doi.org/10.1515/pac-2019-0906>.

- [4] I. Kuselman, F.R. Pennechi, R.J.N.B. da Silva, D.B. Hibbert, How many shades of grey are in conformity assessment due to measurement uncertainty? *J Phys: Conf Series* 1420 (2019) 012001. <https://doi.org/10.1088/1742-6596/1420/1/012001>.
- [5] Ural Research Institute for Metrology - Affiliated Branch of D.I. Mendeleev Institute for Metrology (VNIIM- UNIIM), Ekaterinburg, Russia. <http://www.uniim.ru/> (accessed 6 May 2020).
- [6] ISO Guide 35, Reference materials – Guidance for characterization and assessment of homogeneity and stability, ISO, Geneva, 2017.
- [7] Acros Organics, Geel, Belgium. <http://www.acros.com/> (accessed 20 May 2020).
- [8] The Federation Agency for Technical Regulation and Metrology (Rosstandard), State verification scheme of measuring instruments for contents of inorganic components in liquid and solid substances and materials, Moscow, 2018 (in Russ). http://uniim.ru/wp-content/uploads/2017/08/gps_get_176_2017.pdf (accessed 11 June 2020).
- [9] GOST 4202-75, Reagents. Potassium Iodate. Specifications, Standardinform, Moscow, 1998 (in Russ).
- [10] G.I. Terentiev, A.V. Sobina, A.J. Shimolin, V.M. Zyskin. Application of coulometric titration for the certification of primary reference materials of pure substances, *Am J Anal Chem* 5 (2014) 559-565. <http://dx.doi.org/10.4236/ajac.2014.59063>.
- [11] A.J. Shimolin, A.V. Sobina, V.M. Zyskin, Purity determination of potassium iodate by high-precision coulometric titration: New measurement procedure implementation, *IEEE* (2017) 17410812. <https://doi.org/10.1109/URALCON.2017.8120729>.
- [12] J. Vogl, H. Kipphardt, S. Richter et al, Establishing comparability and compatibility in the purity assessment of high purity zinc as demonstrated by CCQM-P149 intercomparison, *Metrologia* 55 (2018) 211-221. <https://doi.org/10.1088/1681-7575/aaa677>.
- [13] A.C.P. Osorio, R.C. de Sena, T. de O. Araújo, M.D. de Almeida, Purity assessment using the mass balance approach for inorganic in-house certified reference material production at Inmetro, *Accredit Qual Assur* 24 (2019) 387-394. <https://doi.org/10.1007/s00769-019-01392-w>.
- [14] L.A. Konopelko, P.V. Migal, E.P. Sobina, Development of transfer measurement standards in the form of high-purity metals, *Reference materials* 15/2 (2019) 15–24. <https://doi.org/10.20915/2077-1177-2019-15-2-15-24> (in Russ).

- [15] Guide MI 3560-2016, Federal Agency for Technical Regulation and Metrology (Rosstandard), State system for ensuring the uniformity of measurements - Evaluation of measurement uncertainty of mass fraction of main component in inorganic substances, Ekaterinburg, 2016 (in Russ).
- [16] F. Gagnon, D. Ziegler, M. Fafard, Electrochemical modelling using electroneutrality equation as a constraint. *J Appl Electrochem* 44 (2014) 361–381. <https://doi.org/10.1007/s10800-014-0662-6>.
- [17] E.J.F. Dickinson, J.G. Limon-Petersen, R.G. Compton, The electroneutrality approximation in electrochemistry. *J Solid State Electrochem* 15 (2011) 1335–1345. <https://doi.org/10.1007/s10008-011-1323-x>.
- [18] E.P. Sobina, A.V. Sobina, T.N. Tabatchikova, The Federal Agency for Technical Regulation and Metrology (Rosstandart), Method of determining a mass fraction of the main component in sodium chloride and potassium chloride salts, Patent RU 2686468, 2019 (in Russ). <https://www.fips.ru/iiss/document.xhtml?facesredirect=true&id=975e20dc97b65f050dba1fd3cea05a73> (accessed 11 June 2020).
- [19] R. Bettencourt da Silva, A. Williams (Eds), Eurachem/CITAC Guide: Setting and using target uncertainty in chemical measurement, 2015. <https://www.eurachem.org/index.php/publications/guides/gd-stmu> (accessed 11 June 2020).
- [20] Package *stats* version 4.1.0. R Documentation. <https://stat.ethz.ch/R-manual/R-devel/library/stats/html/integrate.html> (accessed 19 June 2020).
- [21] I. Kuselman, F.R. Pennechi, R.J.N.B. da Silva, D.B. Hibbert, Risk of false decision on conformity of a multicomponent material when test results of the components' content are correlated, *Talanta* 174 (2017) 789-796. <https://doi.org/10.1016/j.talanta.2017.06.073>.
- [22] NIST/SEMATECH, e-Handbook of statistical methods. <https://www.itl.nist.gov/div898/handbook/pmd/section1/pmd144.htm> (accessed 15 July 2020).
- [23] K. Aho, ASBIO package. <https://www.rdocumentation.org/packages/asbio/versions/1.6-5/topics/loess.surf> (accessed 17 July 2020).

Figure 1

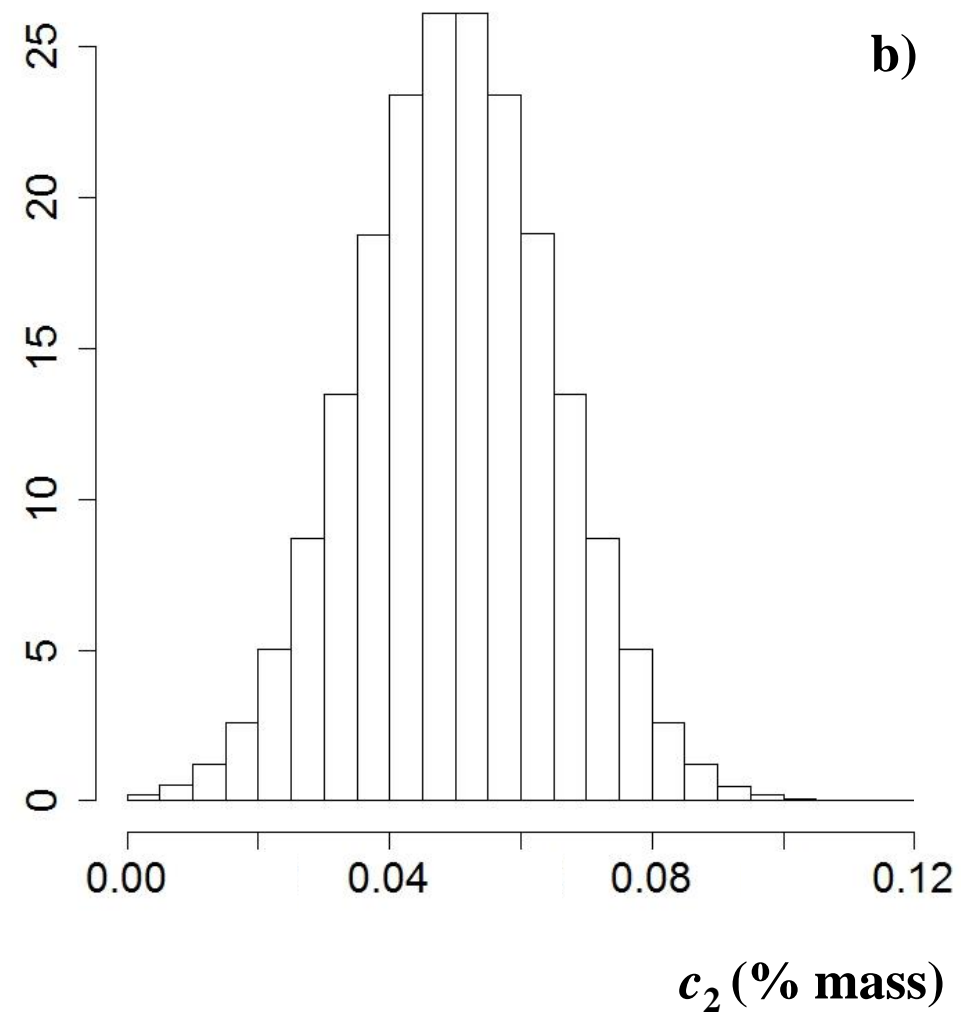
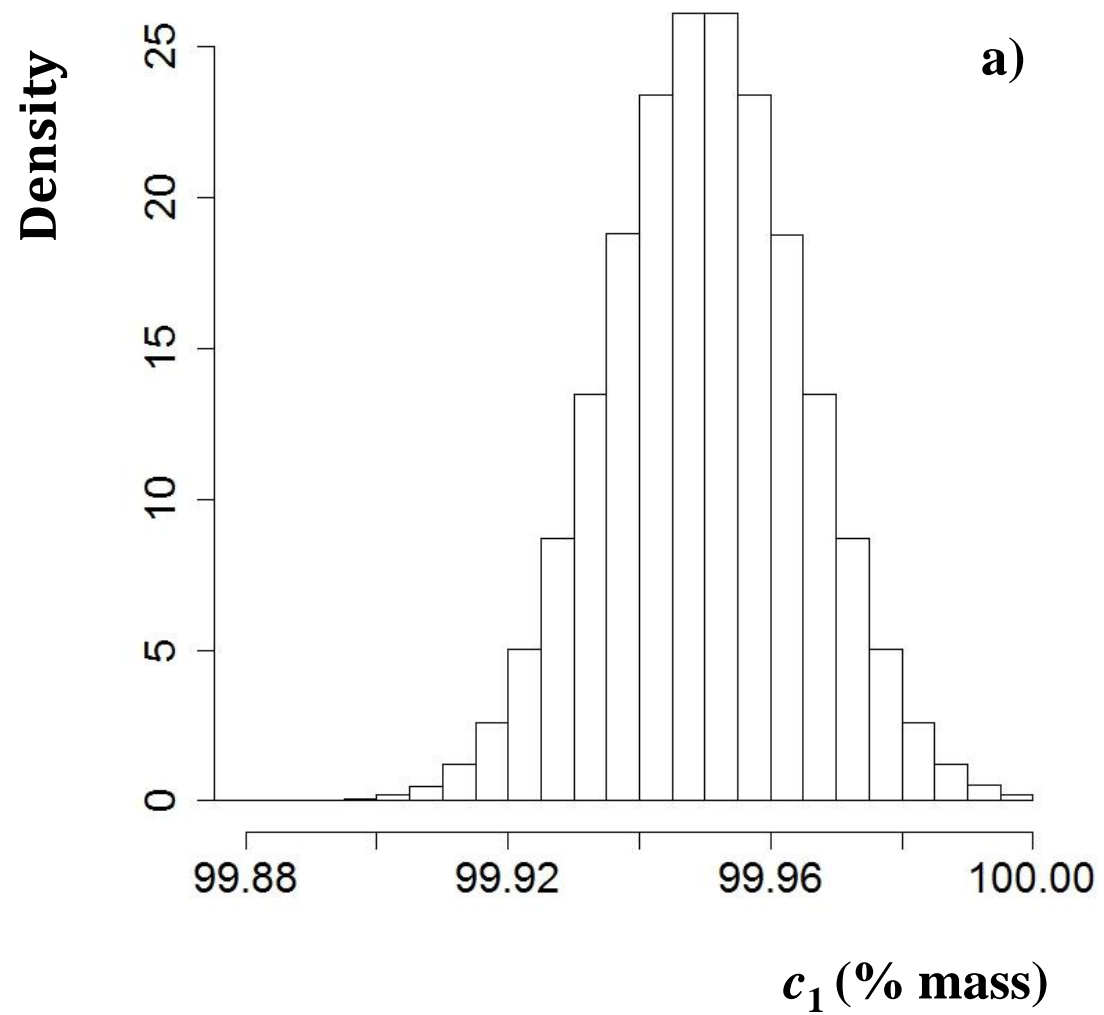


Figure 2

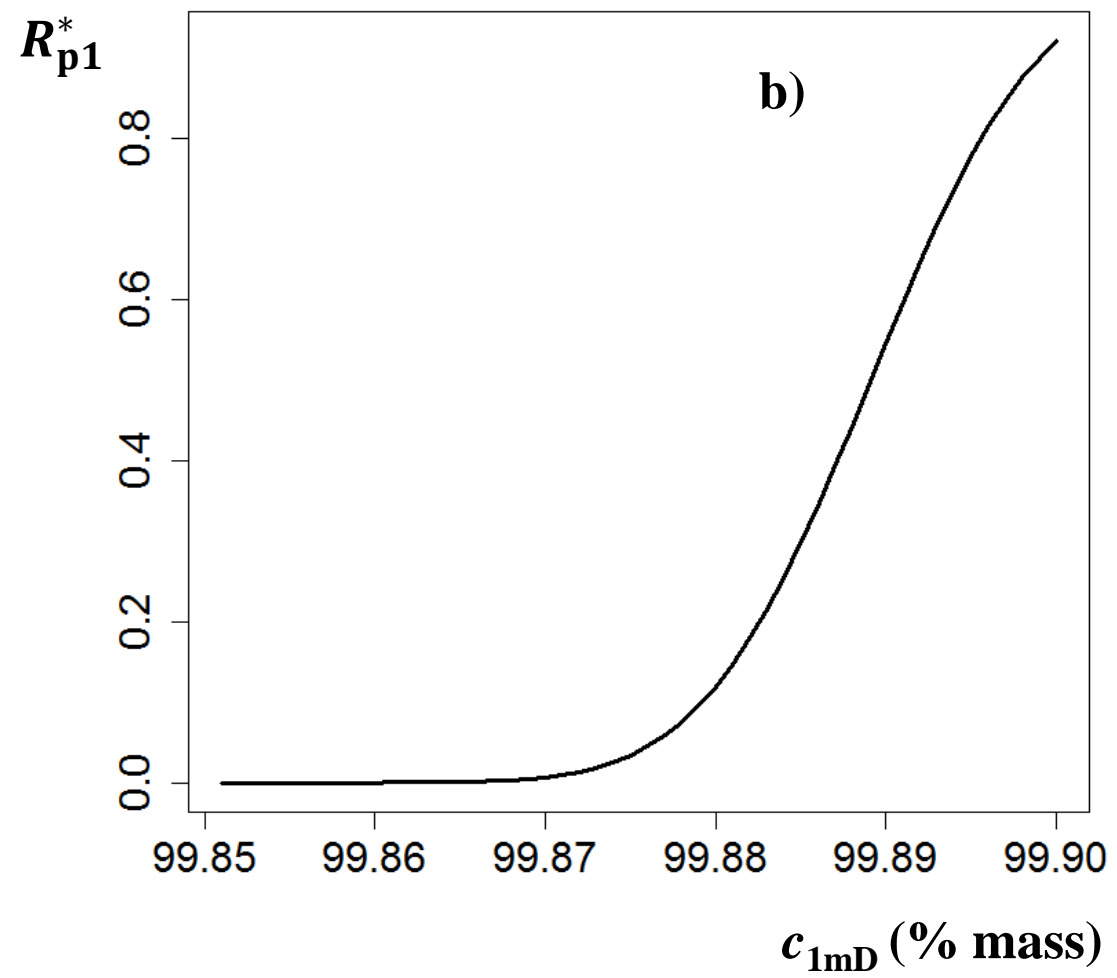
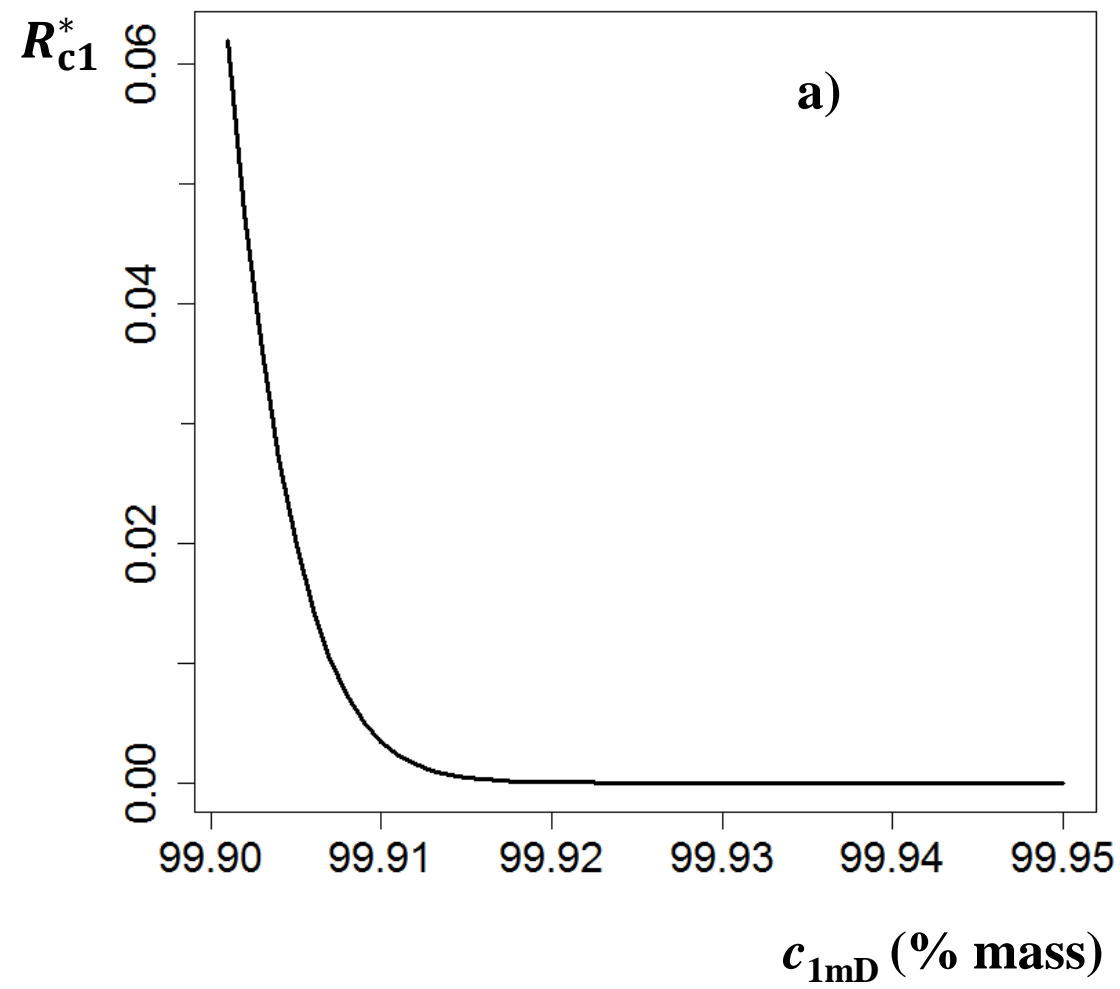
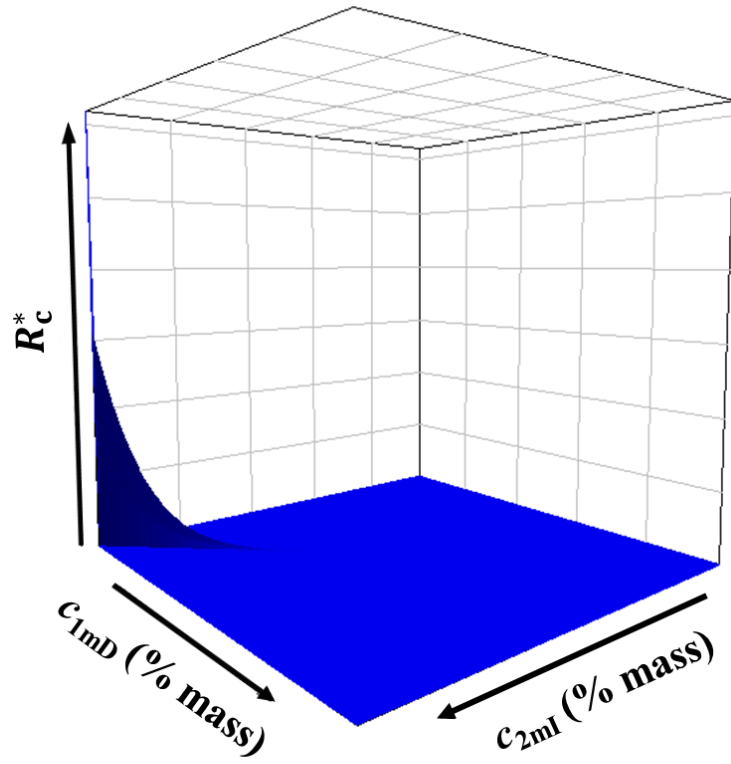


Figure 3

a)



b)

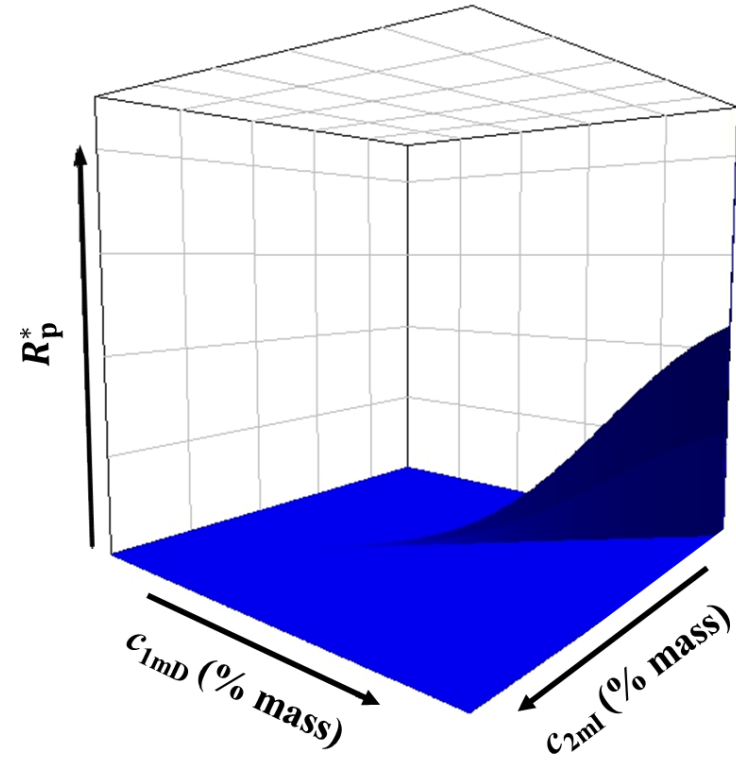


Figure 4

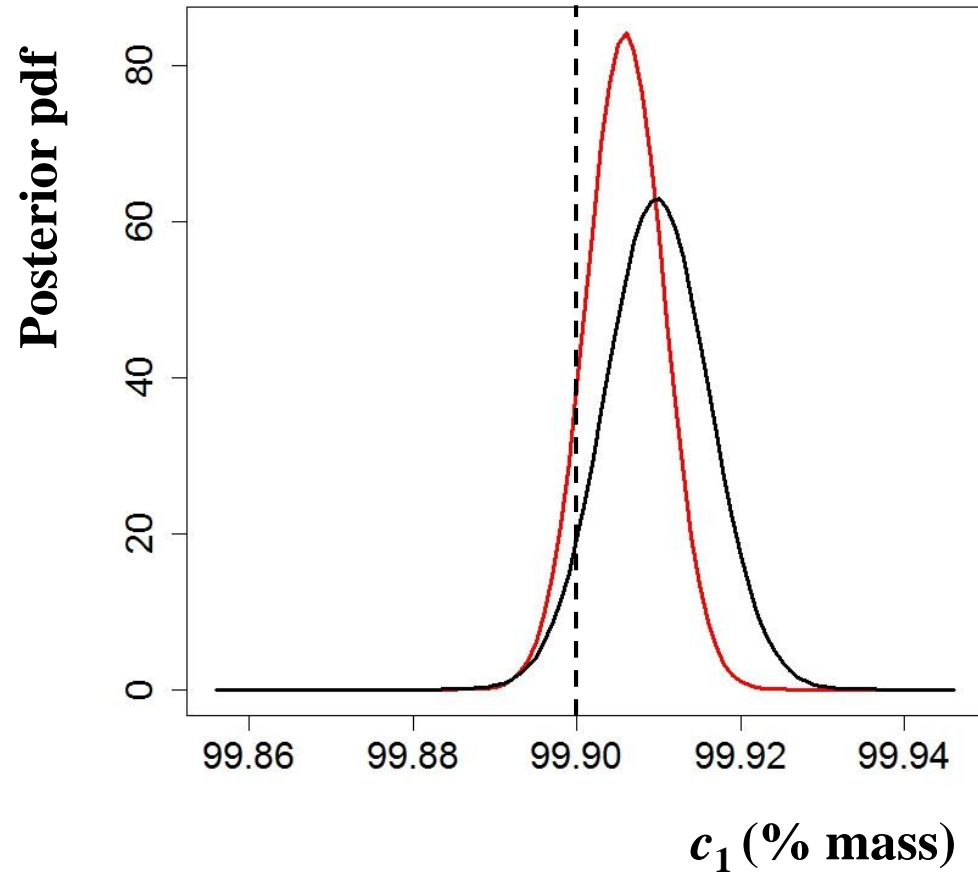
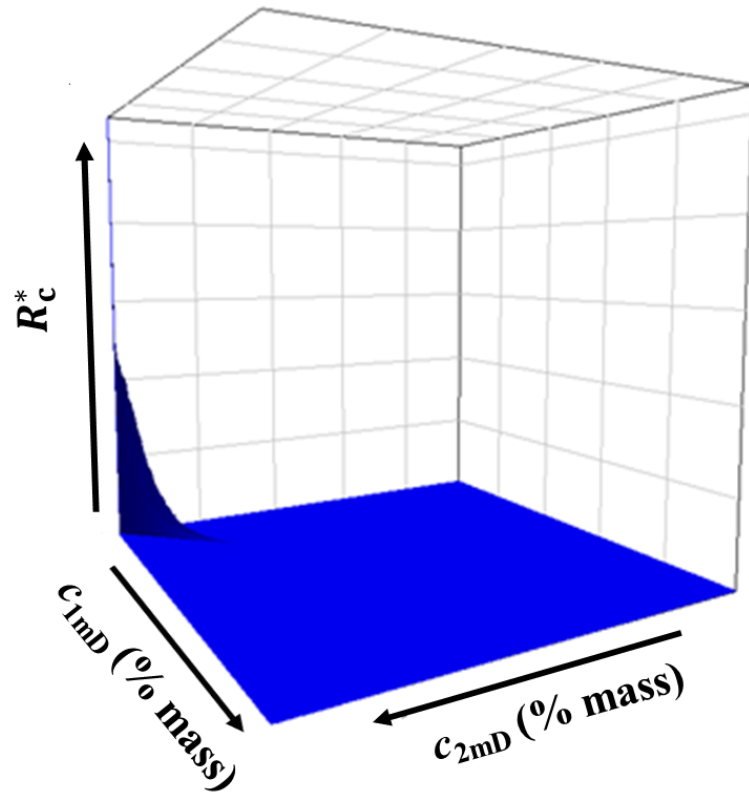


Figure 5

a)



b)

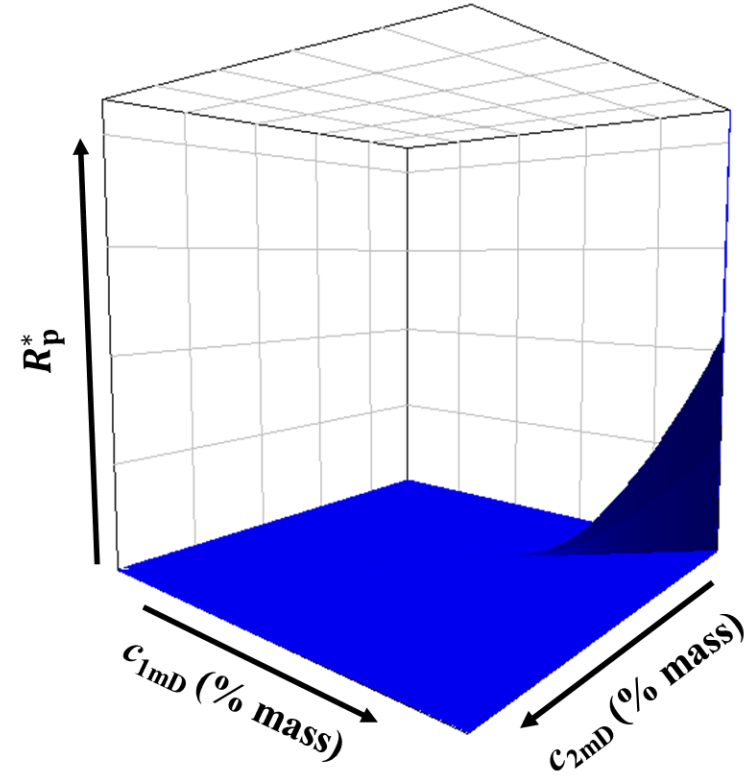
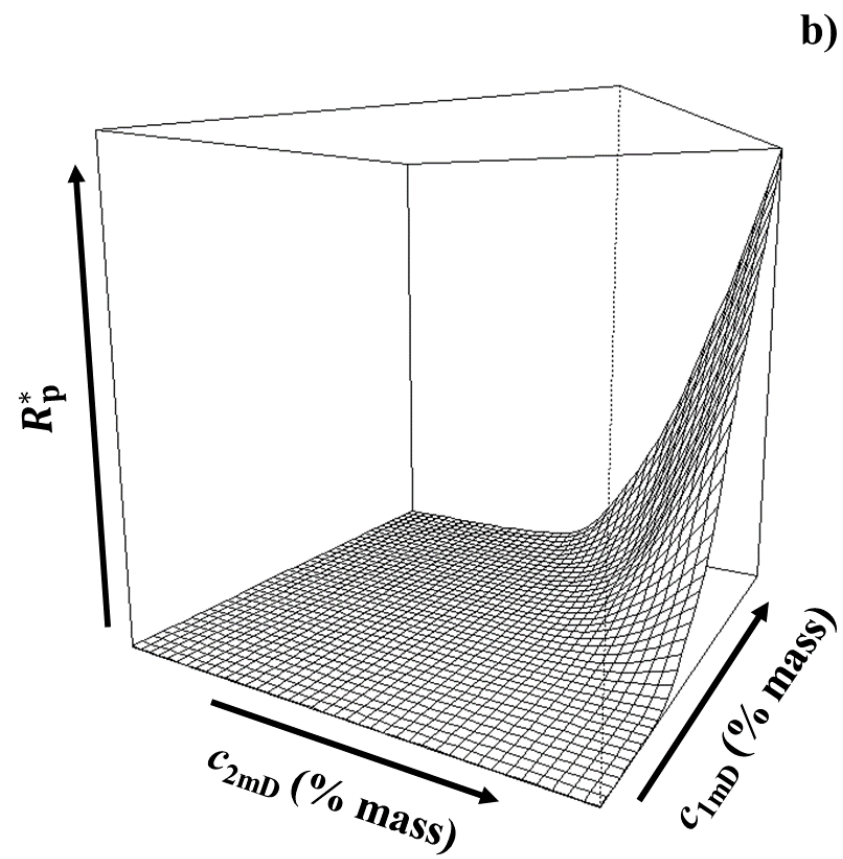
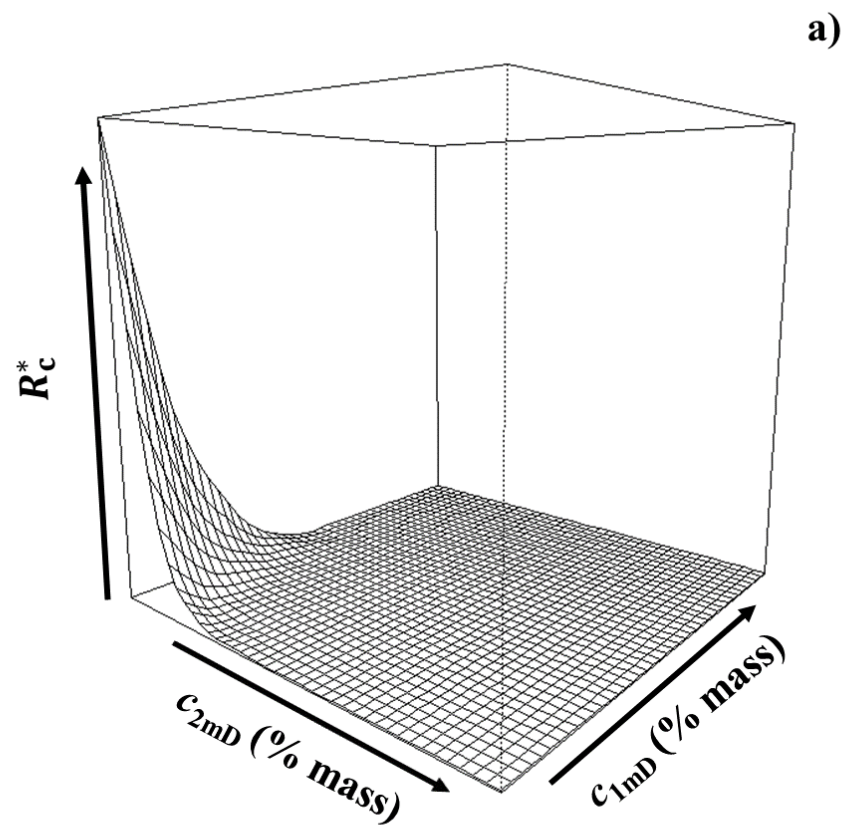


Figure 6



Declaration of interests

The authors declare that they have no known competing financial interests or personal relationships that could have appeared to influence the work reported in this paper.

The authors declare the following financial interests/personal relationships which may be considered as potential competing interests:

Credit Author Statement

Francesca R. Pennecchi: Methodology, Visualization, Formal analysis, Software, Writing – Reviewing and editing; **Ilya Kuselman:** Conceptualization, Project administration, Writing - Original draft preparation; **Aglaia Di Rocco:** Software, Data curation; **D. Brynn Hibbert:** Writing – Reviewing and editing; **Alena Sobina:** Resources: Provision of raw data, Writing – Reviewing and editing; **Egor Sobina:** Validation.